Journal of Materials Chemistry A

RSC Publishing

PAPER

View Article Online
View Journal | View Issue

Cite this: J. Mater. Chem. A, 2013, 1, 1976

Efficient catalytic conversion of ammonia borane to borazine and its use for hexagonal boron nitride (white graphene)†

Sung-Kwan Kim,‡[a] Hyunjin Cho,‡[bd] Myung Jong Kim,*[b] Hee-Jun Lee,[a] Jin-hyung Park,[a] Young-Boo Lee,[c] Hwan Chul Kim,[d] Chang Won Yoon,[e] Suk Woo Nam[e] and Sang Ook Kang*[a]

Received 19th October 2012
Accepted 30th November 2012

DOI: 10.1039/c2ta00758d

www.rsc.org/MaterialsA

Nickel nanoparticles (NiNPs) prepared in tetraglyme (TG) efficiently catalyzed the conversion of ammonia borane (AB, NH_3BH_3) to borazine ($B_3N_3H_6$). Under the optimized conditions, 3 mol% of the NiNPs were introduced into a 1.5 M AB solution in TG and held at 80 °C for 6 h under a dynamic vacuum that was maintained at 30 torr. Borazine was isolated through a series of −45 °C, −78 °C, and −196 °C traps to give (−78 °C trap) pure borazine in 53% yield. The borazine produced was then utilized as a molecular precursor for high quality h-BN (white graphene) and large area h-BN sheets were prepared by applying low pressure chemical vapor deposition (LPCVD). Ultra-thin (single to few layers) h-BN was synthesized on Ni foil at the optimal ratio between borazine and NH_3, and the number of layers was tuned by varying the NH_3 partial pressure.

Introduction

Boron nitride has many important applications particularly in high temperature structural and functional materials.[1] Among the various boron nitride structures, hexagonal boron nitride nanosheets (h-BN, also known as white graphene) have attracted much attention since the discovery of graphene in 2004.[2] Although h-BN shows similarly excellent mechanical and thermal properties, its electrical properties are quite different from those of graphene;[3] while graphene is an electrical conductor, h-BN is an insulator with a direct band-gap of ~6 eV. Similar to graphene, its potential application covers a broad area, such as gate dielectric layers,[4] thermal management,[5] light emitters,[6] and transparent and protective coatings.[7] However, preparation of h-BN through the conventional high temperature sintering process appears to be challenging. Therefore, as an alternate approach, the precursor route has been suggested.[8] In this context, borazine ($B_3N_3H_6$)[9] and ammonia borane (AB, $NH_3 \cdot BH_3$)[10] were reported to be promising precursors for h-BN.[11] Most of all, the AB molecule is regarded as a promising candidate to fulfill the requirements for a high-density, air stable, and easy-to-handle BN source material. With its high BN content of 80.4 wt% and the release of $(BHNH)_n$ from AB with a BN content of 92.5 wt% at 150 °C, it possesses outstanding qualities for this application. In this respect, one important obstacle to using pure AB is its exothermic dehydropolymerization (*e.g.* polyaminoborane or cross-linked BN) generating hydrogen, borazine and aminoborane at 60–180 °C, which would limit its use in the chemical vapor deposition process for h-BN.[12]

On the other hand, borazine has an advantage in that it represents a 1 : 1 stoichiometric ratio of boron and nitrogen atoms constituting a single precursor and has a high enough vapor pressure. From the recent work on the formation of borazine from AB in weakly polar solvent diglyme, Autrey *et al.* reported possible traces of DADB (diammoniate of diborane, $[BH_2(NH_3)_2]^+[BH_4]^-$) in a 2 M solution at 50 °C which accelerated the formation of borazine.[13] In highly concentrated AB–triglyme solutions, the kinetics of this borazine formation process was increased by a higher concentration of DADB and BCDB (*B*-(cyclodiborazanyl)aminoborohydride, cyc[NH_2BH_2–NH_2BH]–NH_2BH_3).[14]

Sneddon and Wideman investigated the production of borazine from AB in tetraglyme (TG) solution with the aim of developing procedures that were both efficient and reliable and

[a]Department of Advanced Materials Chemistry, Korea University, Sejong, Chungnam 339-700, South Korea. E-mail: sangok@korea.ac.kr; Fax: +82 44-867-5396; Tel: +82 44-860-1334

[b]Soft Innovative Materials Research Center, Korea Institute of Science and Technology, Eunha-ri San 101, Bongdong-eup, Wanju-gun, Jeollabuk-do 565-905, South Korea. E-mail: myung@kist.re.kr; Fax: +82 63-219-8249; Tel: +82 63-219-8135

[c]Korea Basic Science Institute, 643-18 Keumam-dong, Dukjin-gu, Jeonju, 561-180, South Korea

[d]Department of Organic Materials and Fiber Engineering, Chonbuk National University, Jeonju, 561-756, South Korea

[e]Fuel Cell Center, Korea Institute of Science and Technology, Hawolgok-dong 39-1, Seongbuk-gu, Seoul 136-791, South Korea

† Electronic supplementary information (ESI) available: Experimental details of TEM images of NiNPs and NMR data of the borazine. See DOI: 10.1039/c2ta00758d

‡ These authors contributed equally.

could be readily accomplished with normal laboratory equipment.[15] With small modifications, the basic Callery batch procedure can be adapted for laboratory scale preparations, and they prepared 10–20 g of borazine over a period of 3–4 h in 67% yield at 140–160 °C (Scheme 1).

In spite of the simplicity of the thermal reaction conditions applied, special care should be taken especially for the large scale synthesis due to its high reaction temperature of 140–160 °C. Consequently, it is desirable to find a suitable catalyst for the reaction to reduce the reaction temperature and to bring the reaction to completion in a shorter period of time.[16]

In this regard, thus far, several efficient catalyst systems have been reported involving rhodium,[17] iridium,[18] platinum,[19] palladium,[20] ruthenium,[21] and nickel.[22] However, Manners *et al.* reported that the isolation of borazine from the reaction mixture proved to be difficult; pure borazine was isolated in only *ca.* 10% yield with the major products being non-volatile, oligomeric species.[17a] If the synthetic conditions are improved, the metal catalysis may be advantageous, which is significant as borazine has been shown to be a useful precursor for BN materials.

As described in a previous report, we found that TG was an efficient growth source for the synthesis of Pd nanoparticles (NPs).[23] This PdNP catalyst was an efficient catalyst for the synthesis of borazine from AB. However, it has been noted that PdNPs were too active in converting AB to borazine and they even activated the produced borazine to polyborazylene which lowered the overall borazine yield. Therefore, more selective and yet economical catalysts are highly sought after. In this study, by adopting the same solvent-mediated nanoparticle synthesis, the related NiNPs were also conveniently prepared from TG solution. The respective nanocatalyst was generally produced by the thermal reaction in TG solvent without surfactants and reductants (Scheme 2). The nanocatalyst could easily be re-dispersed in TG which was used for the synthesis of borazine. These highly reactive and convenient systems are attractive due partly to their heterogeneous nature, which facilitates the separation of the product from the catalyst, and perhaps more importantly due to their relatively low cost and ease of synthesis.

The potential for TG mediated Ni nanoparticles to act as readily available heterogeneous catalysts provided us with a strong incitement to investigate their use in the preparation of borazine (Scheme 3). From the borazine synthesized from AB by Ni nanocatalysts, h-BN was synthesized by low pressure chemical vapor deposition (LPCVD) (Scheme 4). The h-BN formed on the Ni catalyst foil showed a highly crystalline structure with minimal impurities.

$$3NH_3BH_3 \xrightarrow[TG,\ 140\sim160\ ^\circ C]{} B_3N_3H_6 + 6H_2 \quad (1)$$

Scheme 1 Synthesis of borazine from AB.

$$\text{Ni acetate} \xrightarrow[250\ ^\circ C]{TG} \text{Ni nanoparticles} \quad (2)$$

Scheme 2 TG mediated synthesis of Ni nanoparticles from Ni acetate.

$$3NH_3BH_3 \xrightarrow[TG,\ 80\ ^\circ C]{\text{Ni nanoparticles}} B_3N_3H_6 + 6H_2 \quad (3)$$

Scheme 3 Preparation of borazine from AB by metal nanoparticles.

$$B_3N_3H_6 \xrightarrow{LPCVD} \text{Ultra-thin h-BN} \quad (4)$$

Scheme 4 Synthesis of h-BN nanosheets from a borazine precursor using low pressure chemical vapor deposition (LPCVD).

Experimental section

Materials

All experiments were conducted under a nitrogen atmosphere using Schlenk techniques or in an HE-493 dry box (Vacuum Atmosphere Co., Hawthorne, CA, USA). Nickel acetate tetrahydrate ($Ni(OAc)_2\cdot 4H_2O$) was purchased from Aldrich. TG was purchased from Alfa Aesar. AB was prepared as described in the literature.[24] Solvents were dried over Na (TG) below 100 °C and CaH_2 (methanol) and distilled under nitrogen. Deuterated solvents were dried through trap-to-trap distillation from CaH_2 ($CDCl_3$) and Na (C_6D_6) and deoxygenated using three freeze–pump–thaw cycles.

Synthesis of NiNPs

NiNPs were synthesized from $Ni(OAc)_2\cdot 4H_2O$ (**1**). **1** (0.2 g, 0.3 mmol) was added to 20 mL of TG and held at 250 °C for 3 h. The color of the solution changed from green to black. The product was separated by centrifugation. The resulting residue was washed with methanol (50 mL) twice, yielding the NiNPs.

Synthesis of NiNPs deposited on Vulcan XC-72R (NiNPs/VC)

NiNPs/VC were synthesized from $Ni(OAc)_2\cdot 4H_2O$ (**1**) and Vulcan XC-72R (VC). **1** (0.2 g, 0.3 mmol) was added to 20 mL of TG containing VC (0.17 g) and held at 250 °C for 3 h. The product was separated by centrifugation. The resulting residue was washed with methanol (50 mL) twice, yielding 10 wt% NiNPs/VC.

Preparation of borazine from AB using NiNP catalysts

Powdered AB (23.0 g, 747 mmol) dissolved in TG (500 mL) was added to a 2 L, three-necked, round-bottom flask fitted with a thermometer, a reflux condenser, and a solid addition funnel filled with NiNPs (1.31 g, 22.4 mmol, 3 mol%). The exit of the condenser was connected through a series of −45 °C, −78 °C, and −196 °C traps. The system was evacuated and filled with nitrogen gas several times. The NiNPs were added to the flask and the reaction mixture was gradually warmed to 80 °C over the course of 30 min and held at this temperature for 6 h under

a dynamic vacuum that was maintained at 30 torr by the continuous removal of the evolved hydrogen and borazine through the vacuum line. Following the reaction, the borazine that had been retained in the −78 °C trap was further purified by a trap-to-trap distillation to give 10.6 g (131.9 mmol, yield 53.0%). After completion of the reaction and isolation of borazine, the ^{11}B NMR spectrum of the remains of the reaction mixture showed *B*-(cyclodiborazanyl)aminoborohydride (BCDB), as indicated by the peaks at −5.0, −10.9, and −24.0 ppm, cyclotriborazane (CTB) at −10.0 ppm, and polyborazylene at 25–30 ppm.[14]

h-BN growth procedure

Hexagonal boron nitride nanosheets (h-BN) called white graphene were synthesized using low pressure chemical vapor deposition (LPCVD). The nickel thin film (25 μm thick, Alfa Aesar) was used as the metal catalyst substrate and the Ni film was treated by chemical mechanical polishing. Then, the metal catalyst substrate was placed at the middle position in a small quartz tube in the CVD system. The furnace of the CVD system was heated up to 1000 °C at a rate of 10 °C min^{-1} under a hydrogen atmosphere with a flow rate of 9 sccm with a pressure of 118 mtorr. Before synthesizing h-BN, the nickel film was annealed at 1000 °C for 30 min under the same conditions when the CVD furnace was heated in order to make the nickel grains grow and obtain a smooth surface. After annealing, the flow of hydrogen gas into the quartz tube in the CVD system was stopped. Subsequently, h-BN was synthesized for 10 minutes using borazine and ammonia under high vacuum conditions by operating a turbo pump. The operating pressure was approximately 1–5 mtorr. Then, 1–12 sccm of borazine and 1–10 sccm of ammonia were introduced simultaneously in order to form hexagonal BN structures. After synthesizing h-BN, the flow of borazine and ammonia gas into the quartz tube in the CVD system was stopped. Subsequently, the furnace of the CVD system was cooled down to room temperature under a hydrogen atmosphere with a flow rate of 9 sccm.

Transfer

Once the synthesis was completed, h-BN was transferred onto the various substrates and TEM grids for analysis with the graphene transfer method. PMMA (polymethyl methacrylate) was spun on the h-BN/nickel foil at 4200 rpm for 40 seconds, followed by etching the nickel foil with nickel etchant ($FeCl_3$). The film of PMMA/h-BN was washed three times with deionized water for 20 minutes each. Then, the PMMA/h-BN film was transferred onto a 300 nm SiO_2/Si substrate and finally PMMA was removed using acetone.

Characterization

h-BN was analyzed with a scanning electron microscopy instrument (S-4700, HITACHI) and a Raman microscopy instrument (Horiba). A transmission electron microscope instrument (JEM-2200FS) in conjunction with electron energy loss spectroscopy (EELS) and nano-beam electron diffraction (NBED) was used in order to analyze the chemical elements and structure of the h-BN nanosheets, respectively. The NBED measurements were performed using a JEM-2200FS microscope operated at 200 kV with a 5 μm condenser aperture, which gives rise to a semi-convergence angle of under 0.1 mrad.

Results and discussion

In this study, first, we investigated the potential utility of TG as a growth source for producing NiNPs for organonickel complexes. Herein, we present a facile TG-mediated synthesis of NiNPs in the absence of extra reducing agents or a capping agent. Among the various nickel precursors, $Ni(OAc)_2\cdot 4H_2O$ (**1**) showed the best TG solubility and therefore was used for the synthesis of the NPs. At 250 °C, **1** was quantitatively converted to NiNPs in the presence of TG.

The thermal decomposition of **1** has been the subject of several previous studies.[25] On linear heating, **1** first releases water at *ca.* 120 °C. On continued heating, the subsequent decomposition of **1** at *ca.* 340 °C leads directly to the formation of either NiO or Ni.[26] It was also reported that the evolution of some CH_3COOH occurs and, on continued heating, anion breakdown occurs yielding CO_2, CO, acetic anhydride and acetone.[27]

In Fig. 1(a), the TEM analysis of the NiNPs prepared in TG at 250 °C showed spherical 5 nm size nanoparticles. On the other hand, agglomerates in the size range of 100–200 nm coexisted with the smaller 5 nm size NiNPs (Fig. S1†). This is explained by the weak binding of TG on the surface of the NiNPs.

The diffraction peaks at 2θ values of 39.1°, 41.5°, 44.5°, 58.5°, 71.1°, and 78.0° in Fig. 1(b) are assigned to the (010), (002), (011), (012), (110), and (103) planes of hcp Ni (JCPDS no. 45-1027). On the other hand, small peaks are observed at 52.0° and 76.4° which are assigned to the (200) and (220) planes of fcc Ni (JCPDS no. 04-0850), respectively. It should be noted that the main peak (111) of fcc Ni overlaps with that of the hcp Ni (011).[28]

These screened NiNPs were found to promote the formation of borazine relative to the background reaction, as shown in Fig. 2(a).[29] The reaction of AB was found to proceed vigorously at low temperature (80 °C) when the NiNPs were introduced. It took 6 h to complete the reaction at 80 °C with the NiNPs. Borazine was obtained in 53% yield after purification, which is a substantial improvement over the yield obtained when the reaction was performed without catalysts at 80 °C (19% yield). The NiNPs, besides increasing both the rate and conversion of

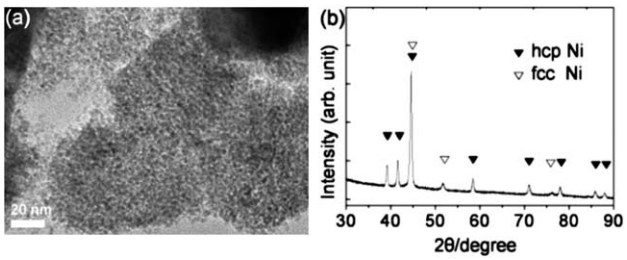

Fig. 1 (a) TEM image of NiNPs prepared from $Ni(OAc)_2\cdot 4H_2O$ (**1**). Scale bar = 20 nm. (b) XRD pattern of NiNPs prepared from **1**.

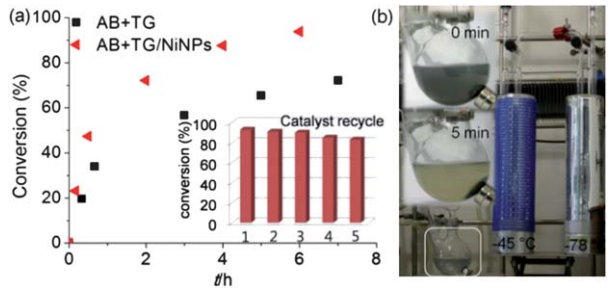

Fig. 2 (a) Conversion of AB to borazine by NiNPs and catalyst recycle (inset). (b) Attraction of NiNPs by a magnetic bar in reaction solution.

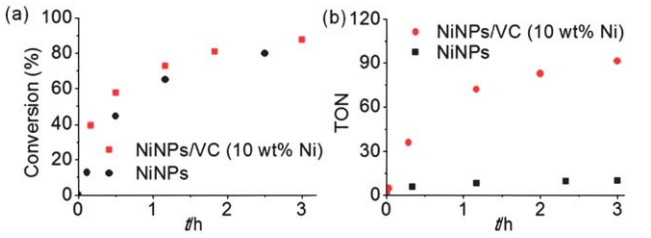

Fig. 3 (a) Conversion of AB to borazine by NiNPs and NiNPs/VC. (b) TON (turnover number: mol of borazine/mol of Ni) for NiNPs and NiNPs/VC (10 wt% Ni).

AB to borazine, were found to have a highly beneficial effect of significantly reducing foaming during borazine synthesis. This effect resulted from the feature that NiNPs play a role as boiling chips.

To understand the underlying mechanistic steps responsible for the formation of borazine by the NiNPs, we coupled the synthesis experiments with *ex situ* ^{11}B NMR spectroscopy as shown in Fig. S2.† The ^{11}B NMR analysis of the reaction mixtures in TG demonstrated the initial formation of BCDB. Following the initial growth of BCDB, we observed new resonances due to borazine. Further dehydrogenation showed the simultaneous decay of BCDB and formation of borazine, as identified by Sneddon *et al.*[30] and Shaw *et al.*[13b]

Our synthesis method of NiNPs is convenient, requiring only a single chemical reagent. We believe that their broad size distribution and irregular shape come from the weak interaction between the nickel metals and TG. It has been suggested that the catalytic activity is dependent on the number of low coordination number sites available on the surface of the nanoparticles and irregular NiNPs bear more of these sites than flatter and more faceted ones.[31] If these low coordination number corners and/or edge positions are implicated as active sites for the activation of AB, then their relatively higher occurrence in the NiNPs generated in this study could account for their superior catalytic performance.

An advantageous feature of the use of NiNPs is their recyclability in that they can be collected using a magnet after the reaction. As can be seen in Fig. 2(b), the dark-colored dispersion turned transparent after 5 min, while all of the particles assembled at the side of the flask next to the magnet. After the catalytic dehydrogenation and separation of the NiNPs, a visible layer appeared to coat the catalyst. This coating was removed by simple immersion in methanol and the NiNPs retrieved from the solvent exhibited close to their original catalytic activity, which was sustainable up to the fifth cycle without any discernible catalytic loss as shown in Fig. 2(a).

Moreover, the confinement of the NiNPs in ordered carbon support materials induces high catalytic activity. It is noteworthy that 10 wt% NiNPs/Vulcan XC-72R (metal loading 0.3 mol%) show similar catalytic activity to that of the NiNPs (metal loading 3.0 mol%) by themselves (Fig. 3(a)). These results suggest that NiNPs on a carbon support bear more active sites than the NiNPs, which finally results in enhanced catalytic performance, with an initial turnover frequency (TOF) of 62 h^{-1} as compared to 7 h^{-1} for the metallic catalyst NiNPs, as shown in Fig. 3(b).

With this convenient AB to borazine route in hand, we pursued precursor routes for the synthesis of h-BN and low pressure CVD (LPCVD) was adopted for the sake of improving the controllability. LPCVD has an advantage over APCVD (atmospheric CVD) in that it provides for a uniform film thickness stemming from the surface reaction limited kinetics.[32] Ammonia (NH_3) gas was used not only for controlling the kinetics or achieving amorphous etching, but also for the purpose of providing extra nitrogen during the growth process due to the limited solubility of nitrogen in the Ni catalyst. Though borazine provides boron and nitrogen with a 1 : 1 ratio, the ability of Ni to dissolve each atom is different. Solubility of boron in Ni is much higher than that of nitrogen. Considering h-BN formation occurs at the Ni surface, highly concentrated nitrogen has better chance to combine with dissolved boron by diffusion to the surface.[33] Also, this tendency was observed in BN nanotube CVD synthesis with borazine. Boron nitride could not be synthesized without NH_3, which is an extra source of nitrogen.[34]

As shown in Fig. 4, single to few-layered h-BN was synthesized at the optimized ratio between borazine and ammonia (borazine: 1 sccm, NH_3: 8 sccm). From the TEM images taken from the edges of h-BN, the wall structures of h-BN were clearly identified and the interlayer spacing of h-BN was ~0.34 nm.

In order to obtain the diffraction pattern from clean h-BN, the nano-beam electron diffraction (NBED) method was used. The NBED method has been proven to be a useful tool for the structural analysis of nanomaterials.[35–38] NBED refers to

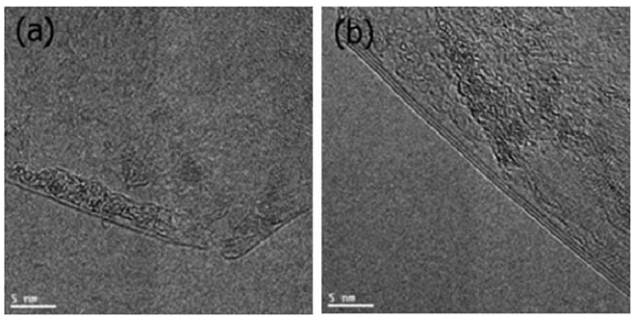

Fig. 4 TEM images of (a) single-layered and (b) few-layered h-BN.

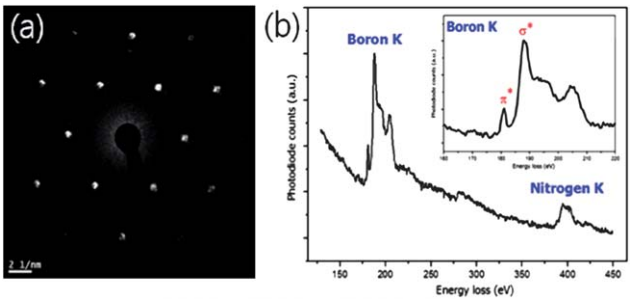

Fig. 5 (a) Nanobeam electron diffraction (NBED) data and (b) EELS data of h-BN.

acquiring a diffraction area of the size of a few nanometers while maintaining a small convergence angle (<0.1 mrad).

As shown in Fig. 5(a), the grown h-BN has an unambiguous hexagonal structure with a [0001] orientation. The EELS data in Fig. 5(b) show sharp boron and nitrogen K edges that are characteristic of the sp^2 hybridized atoms of boron nitride, while the carbon K edge resulting from contamination is at the noise level.

h-BN grown on Ni foil could be transferred to various substrates including Si wafers, glass substrates, and PET using a similar method to that reported for graphene.[39] The piece of Si wafer, onto which the h-BN was transferred, developed a whitish color indicating a large band gap, as shown in Fig. 6(a). The Raman spectrum was obtained from the h-BN/SiO_2/Si (h-BN on SiO_2/Si wafer) sample. The thickness of the h-BN for Raman analysis was ~2.7 nm measured by AFM. It clearly showed a peak at 1366.5 cm^{-1} indicating the E_{2g} mode stretching of hexagonal boron nitride.[40] No peaks indicating the presence of BN soot (1322–1350 cm^{-1}) or c-BN (1304 cm^{-1}) were observed, as shown in Fig. 6(b).

Based on the advantage of borazine as a single chemical precursor, layer by layer control was attempted by varying the NH_3 gas flow rate. While the borazine flow rate was fixed at 1 sccm, the NH_3 flow rate was regulated at 2, 4, 6, or 8 sccm for each experiment. As shown in Fig. 7, there was an observed tendency that the number of layers gradually decreased with increasing flow rate of NH_3. However, this does not mean that we have absolute layer by layer control over a large area, because the growth rate of h-BN differs in each grain of the Ni foil. Absolute control over the number of layers is still an open issue.

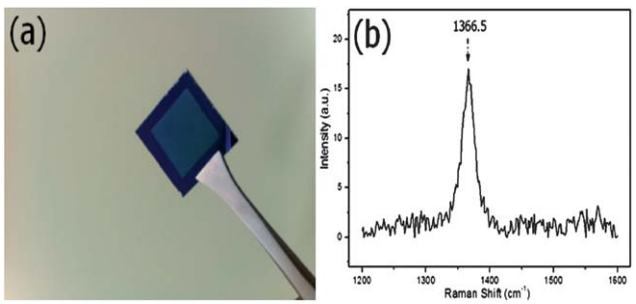

Fig. 6 (a) Photographic image and (b) Raman data of a transferred h-BN.

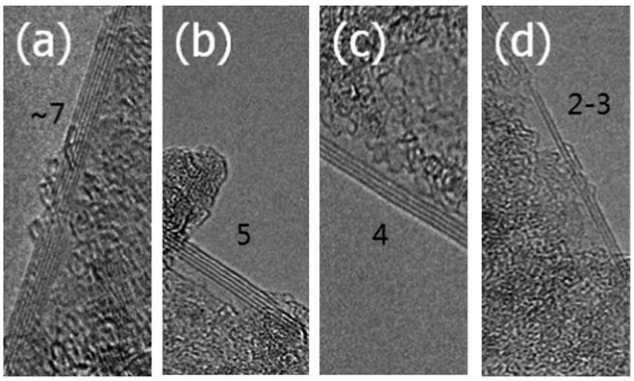

Fig. 7 TEM images of grown h-BNs at different flow rates of (a) 2 sccm, (b) 4 sccm, (c) 6 sccm, and (d) 8 sccm.

Conclusions

Pure borazine was effectively synthesized by an efficient method utilizing NiNPs. The lower synthetic temperature proved the catalytic action of the NiNPs. The use of borazine as a stable precursor in conjunction with LPCVD provides a high degree of control for the synthesis of h-BN. Considering the TEM, EELS, NBED, and Raman spectrum, high quality h-BN with a large area was synthesized on Ni foil, and the number of layers could be tuned by varying the NH_3 partial pressure.

Acknowledgements

This work was supported by a grant from the Korea Institute of Science and Technology (KIST) Institutional Program and the Converging Research Center Program funded by the Ministry of Education, Science and Technology (2012K001429). This work was also supported by the New & Renewable Energy Technology Development Program of the Korea Institute of Energy Technology Evaluation and Planning (KETEP) grant funded by the Korea government Ministry of Knowledge Economy (20113030040020). We also acknowledge the Korea Basic Science Institute (KBSI) for TEM experiments.

Notes and references

1 J. Eichler and C. Lesniak, *J. Eur. Ceram. Soc.*, 2008, **28**, 1105.
2 K. S. Novoselov, A. K. Geim, S. V. Morozov, D. Jiang, Y. Zhang, S. V. Dubonos, I. V. Grigorieva and A. A. Firsov, *Science*, 2004, **306**, 666.
3 A. Zunger, A. Katzir and A. Halperin, *Phys. Rev. B: Solid State*, 1976, **13**, 5560.
4 I. Meric, C. Dean, A. Young, J. Hone, P. Kim and K. L. Shepard, *IEEE Int. Electron Devices Meet.*, 2010, 556.
5 C. W. Chang, A. M. Fennimore, A. Afanasiev, D. Okawa, T. Ikuno, H. Garcia, D. Li, A. Majundar and A. Zettl, *Phys. Rev. Lett.*, 2006, **97**, 085901.
6 Y. Kubota, K. Watanabe, O. Tsuda and T. Taniguchi, *Science*, 2007, **317**, 932.
7 A. Pakdel, C. Zhi, Y. Bando, T. Nakayama and D. Golberg, *ACS Nano*, 2011, **5**, 6507.

8 P. Colombo, *J. Eur. Ceram. Soc.*, 2008, **28**, 1389.
9 (*a*) Y. Shi, C. Hamsen, X. Jia, K. K. Kim, A. Reina, M. Hofmann, A. L. Hsu, K. Zhang, H. Li, Z.-Y. Juang, M. S. Dresselhaus, L.-J. Li and J. Kong, *Nano Lett.*, 2010, **10**, 4134; (*b*) M. Coroso, W. Auwarter, A. Tamai, T. Greber and J. Osterwalder, *Science*, 2004, **303**, 217.
10 (*a*) L. Song, L. Ci, H. Lu, P. B. Sorokin, C. Jin, J. Ni, A. G. Kvashnin, D. G. Kavashnin, J. Lou, B. I. Yakobson and P. M. Ajayan, *Nano Lett.*, 2010, **10**, 3209; (*b*) K. H. Lee, H.-J. Shin, J. Lee, I.-Y. Lee, G.-H. Kim, J.-Y. Choi and S.-W. Kim, *Nano Lett.*, 2012, **12**, 714; (*c*) Y.-H. Lee, K.-K. Liu, A.-Y. Lu, C.-Y. Wu, C.-T. Lin, W. Zhang, C.-Y. Su, C.-L. Hsu, T.-W. Lin, K.-H. Wei, Y. Shi and L.-J. Li, *RSC Adv.*, 2012, **2**, 111.
11 S. Seghi, J. Lee and J. Economy, *Carbon*, 2005, **43**, 2035.
12 K. K. Kim, A. Hsu, X. Jia, S. M. Kim, Y. Shi, M. Hofmann, D. Nezich, J. F. Rodriguez-Nieva, M. Dresselhaus, T. Palacios and J. Kong, *Nano Lett.*, 2012, **12**, 161.
13 (*a*) A. C. Stowe, W. J. Shaw, J. C. Linehan, B. Schmid and T. Autrey, *Phys. Chem. Chem. Phys.*, 2007, **9**, 1831; (*b*) W. J. Shaw, J. C. Linehan, N. K. Szymczak, D. J. Heldebrant, C. Yonker, D. M. Camaioni, R. T. Baker and T. Autrey, *Angew. Chem., Int. Ed.*, 2008, **47**, 7493.
14 J. F. Kostka, R. Schellenberg, F. Baitalow, T. Smolinka and F. Mertens, *Eur. J. Inorg. Chem.*, 2012, 49.
15 T. Wideman and L. G. Sneddon, *Inorg. Chem.*, 1995, **34**, 1002.
16 J.-S. Li, C.-R. Zhang, B. Li, F. Cao and S.-Q. Wang, *Eur. J. Inorg. Chem.*, 2010, 1763.
17 (*a*) C. A. Jaska, K. Temple, A. J. Lough and I. Manners, *Chem. Commun.*, 2001, 962; (*b*) C. A. Jaska and I. Manners, *J. Am. Chem. Soc.*, 2004, **126**, 9776; (*c*) C. A. Jaska, T. J. Clark, S. B. Clendenning, D. Grozea, A. Turak, Z.-H. Lu and I. Manners, *J. Am. Chem. Soc.*, 2005, **127**, 5116.
18 M. C. Denney, V. Pons, T. J. Hebden, M. Heinekey and K. I. Goldberg, *J. Am. Chem. Soc.*, 2006, **128**, 12048.
19 R. P. Shrestha, H. V. K. Diyabalanage, T. A. Semelsberger, K. C. Ott and A. K. Burrell, *Int. J. Hydrogen Energy*, 2009, **34**, 2616.
20 Ö. Metin, S. Duman, M. Dinç and S. Özkar, *J. Phys. Chem. C*, 2011, **115**, 10736.
21 (*a*) N. Blaquiere, S. Diallo-Garcia, S. I. Gorelsky, D. A. Black and K. Fagnou, *J. Am. Chem. Soc.*, 2008, **130**, 14034; (*b*) M. Käss, A. Friedrich, M. Drees and S. Schneider, *Angew. Chem., Int. Ed.*, 2009, **48**, 905.
22 (*a*) R. J. Keaton, J. M. Blacquiere and R. T. Baker, *J. Am. Chem. Soc.*, 2007, **129**, 1844; (*b*) A. P. M. Robertson, R. Suter, L. Chabanne, G. R. Whittell and I. Manners, *Inorg. Chem.*, 2011, **50**, 12860; (*c*) B. L. Conley, D. Guess and T. J. Williams, *J. Am. Chem. Soc.*, 2011, **133**, 14212.
23 S.-K. Kim, T.-J. Kim, T.-Y. Kim, G. Lee, J. T. Park, S. W. Nam and S. O. Kang, *Chem. Commun.*, 2012, **48**, 2021.
24 P. V. Ramachandran and P. D. Gagare, *Inorg. Chem.*, 2007, **46**, 7810.
25 (*a*) P. Baraldi, *Spectrochim. Acta, Part A*, 1982, **38**, 51; (*b*) M. Afzal, P. K. Butt and H. Ahmad, *J. Therm. Anal.*, 1991, **37**, 1015; (*c*) A. M. Gadalla and H. F. Yu, *Thermochim. Acta*, 1990, **164**, 21; (*d*) G. A. M. Hussein, A. K. H. Nohman and K. M. A. Attyia, *J. Therm. Anal.*, 1994, **42**, 1155; (*e*) N. Nishizawa, T. Kishikawa and H. Minami, *J. Solid State Chem.*, 1999, **146**, 39; (*f*) A. K. Galwey, S. G. McKee and T. R. B. Mitchell, *React. Solids*, 1988, **6**, 173.
26 J. C. De jesus, I. González, A. Quevedo and T. Puerta, *J. Mol. Catal. A: Chem.*, 2005, **228**, 283.
27 Y. Guo, M. U. Azmat, X. Liu, J. Ren, Y. Wang and G. Lu, *J. Mater. Sci.*, 2011, **46**, 4606.
28 M. A. Mohamed, S. A. Halawy and M. M. Ebrahim, *J. Anal. Appl. Pyrolysis*, 1993, **27**, 109.
29 It is notable that there is also significant dehydrogenation in the absence of the catalyst. In this report, the efficient borazine formation from AB resulted from a synergistic effect of NiNPs and thermolytic dehydrogenation in TG solvent.
30 (*a*) D. W. Himmelberger, L. R. Alden, M. E. Bluhm and L. G. Sneddon, *Inorg. Chem.*, 2009, **48**, 9883; (*b*) D. W. Himmelberger, C. W. Yoon, M. E. Bluhm, P. J. Carroll and L. G. Sneddon, *J. Am. Chem. Soc.*, 2009, **131**, 14101; (*c*) M. E. Bluhm, M. G. Bradley, R. Butterick III, U. Kusari and L. G. Sneddon, *J. Am. Chem. Soc.*, 2006, **128**, 7748; (*d*) W. R. H. Wright, E. R. Berkeley, L. R. Alden, R. T. Baker and L. G. Sneddon, *Chem. Commun.*, 2011, **47**, 3177.
31 L. Kesavan, R. Tiruvalam, M. H. A. Rahim, M. I. B. Saiman, D. I. Enache, R. L. Jenkins, N. Dimitratos, J. A. Lopez-Sanchez, S. H. Taylor, D. W. Knight, C. J. Kiely and G. J. Hutchings, *Science*, 2011, **331**, 195.
32 A. S. Grove, *Physics and Technology of Semiconductor Devices*, John Wiley and Sons, New York, 1967.
33 P. C. Yang, J. T. Prater, W. Liu, J. T. Glass and R. F. Davis, *J. Electron. Mater.*, 2005, **34**, 1558.
34 S. Chatterjee, M. J. Kim, D. N. Zakharov, S. M. Kim, E. A. Stach, B. Maruyama and L. G. Sneddon, *Chem. Mater.*, 2012, **24**, 2872.
35 J. C. Spence and J. M. Zuo, *Electron Microdiffraction*, Plenum Press, New York, 1992.
36 J. M. Cowley, *Microsc. Res. Tech.*, 1999, **46**, 75.
37 J. M. Zuo, I. Vartanyants, M. Gao, R. Zhang and L. A. Nagahara, *Science*, 2003, **300**, 1419.
38 S. Amelinckx, A. Lucus and P. Lambin, *Rep. Prog. Phys.*, 1999, **62**, 1471.
39 X. Li, Y. Zhu, W. Cai, M. Borysiak, B. Han, D. Chen, R. D. Piner, L. Colombo and R. S. Ruoff, *Nano Lett.*, 2009, **9**, 4359.
40 R. V. Gorbachev, I. Riaz, R. R. Nair, R. Jalil, L. Britnell, L. Britnell, B. D. Belle, E. W. Hill, K. S. Novoselov, K. Watanabe, T. Taniguchi, A. K. Geim and B. Blake, *Small*, 2011, **7**, 465.